New Mode of Ion Size Discrimination for Group 2 Metals Using Poly(pyrazolyl)borate Ligands. Control of Stability and Structure of Chelate Complexes by Intraligand Contact

Yoshiki Sohrin,*,† Hisao Kokusen,† Sorin Kihara,† Masakazu Matsui,† Yoshihiko Kushi,‡ and Motoo Shiro§

Contribution from the Institute for Chemical Research, Kyoto University, Uji, Kyoto 611, Japan, Institute for Molecular Science, Okazaki National Research Institutes, Myodaiji, Okazaki 444, Japan, and Rigaku Corporation, Matsubara-cho 3-9-12, Akishima, Tokyo 196, Japan

Received October 5, 1992

Abstract: Selectivity of $[H_nB(pz)_{4-n}]^-$ (n = 0–2; pz = pyrazolyl ring) for group 2 metal ions has been studied by liquid–liquid extraction. The dominant extracted species is $[H_nB(pz)_{4-n}]_2M$. Bidentate $[H_2B(pz)_2]^-$ is a weak extracting reagent for Be^{2+} and Mg^{2+}. Hydrotris(pyrazolyl)borate extracts Be^{2+}, Mg^{2+}, and Ca^{2+} effectively, and Sr^{2+} to some extent. Although $[B(pz)_4]^-$, a potentially tridentate ligand similar to $[HB(pz)_3]^-$, extracts Be^{2+} and Mg^{2+}, the extractability for Ca^{2+} drops drastically. The different selectivity of these ligands cannot be explained on the basis of basicity of the donor atoms. To explore the origin of the selectivity, X-ray crystal structures of the extracted species have been determined. Complexes of $[HB(pz)_3]_2Mg$ (**1**), $[HB(pz)_3]_2Ca$ (**2**), and $[B(pz)_4]_2Mg$ (**3**) have distorted octahedral geometries with each ligand having tridentate coordination. In complex $[B(pz)_4]_2Be$ (**4**), the ligands are bidentate and the geometry about the beryllium atom is distorted tetrahedral. The extracted species of Be^{2+} with $[HB(pz)_3]^-$ changes from $[HB(pz)_3]_2Be$ to $[(HB(pz)_3)BeOH]_3$ (**5**) as the initial concentration of Be^{2+} increases from 10^{-4} to 10^{-2} M. Complex **5** consists of bidentate $[HB(pz)_3]^-$ and a cyclic $[BeOH]_3^{3+}$ moiety which is the dominant species of beryllium in aqueous solution (pH 5). The ^1H NMR spectra show that solution structures of these complexes in $CDCl_3$ are similar to the structures in solid state. Examination of the dimensions of the complexes has revealed that the stability and structure of poly(pyrazolyl)borate complexes of group 2 metals are controlled by intraligand contact between pyrazolyl rings bonded to the central boron atom. This is a novel mode of ion size discrimination by chelating ligands.

Introduction

Discrimination of the ion size is an essential factor in ligand design for selective complexation of metal ions. The size distinction with conventional organic ligands is roughly divided into two types. The first is based on the chelate ring size.[1] The chelate ring size is principally determined by the kind and number of atoms and the order of bonds contained in the ring. For hard metal ions, such as those of group 2 and the lanthanide series, the stability constants of conventional chelating complexes decrease gradually with an increase in the ion size, and the change in the stability constants is affected by the chelate ring size. The second type of ion size discrimination is based on the cavity size of macrocyclic ligands.[2] It is especially obvious in rigid and preorganized macrocycles that the most stable complex is formed when the cation diameter matches the cavity size. The type of distinction of ion size restricts the variety of selectivity patterns for the ions. The creation of a new mode of ion size discrimination is desired to produce a novel pattern of ion selectivity and expand the possibility of metal ion recognition.

In the present work, ion size discrimination for group 2 metals with poly(pyrazolyl)borates, $[H_nB(pz)_{4-n}]^-$ (n = 0–2), has been investigated. While the poly(pyrazolyl)borates that form stable complexes with various metal ions have attracted considerable attention in the field of coordination chemistry,[3] little is known about the selectivity for metal ions.[4] All these ligands are similar in that they form a six-membered MN_4B chelate ring of shallow boat configuration. Both $[HB(pz)_3]^-$ and $[B(pz)_4]^-$ act as a tripodal tridentate or bidentate ligand.[5-7] Liquid–liquid extraction study, however, has demonstrated that the selectivity of poly(pyrazolyl)borates for group 2 metal ions is very different. To explore the origin of the selectivity, X-ray crystal structures of extracted species $[HB(pz)_3]_2Mg$ (**1**), $[HB(pz)_3]_2Ca$ (**2**), $[B(pz)_4]_2Mg$ (**3**), $[B(pz)_4]_2Be$ (**4**), and $[(HB(pz)_3)BeOH]_3$ (**5**) have been determined.[8] It has been found that the selectivity is ascribed to the preferred conformation and bite size (intraligand distance between donor atoms) of the ligands. The poly(pyrazolyl)borates differ from the conventional ligands in that

* Author to whom correspondence should be addressed.
† Kyoto University.
‡ Institute for Molecular Science. Present address: College of Liberal Arts and Sciences, Osaka University, Toyonaka, Osaka 560, Japan.
§ Rigaku Corporation.

(1) (a) Hancock, R. D.; Martell, A. E. *Chem. Rev.* **1989**, *89*, 1875–1914. (b) Hancock, R. D. *Prog. Inorg. Chem.* **1989**, *37*, 187–291.

(2) Izatt, R. M.; Pawlak, K.; Bradshaw, J. S.; Bruening, R. L. *Chem. Rev.* **1991**, *91*, 1721–2085.

(3) (a) Trofimenko, S. *Prog. Inorg. Chem.* **1986**, *34*, 115–210. (b) Han, R.; Parkin, G. *J. Am. Chem. Soc.* **1992**, *114*, 748–757. (c) Kitajima, N.; Fujisawa, K.; Fujimoto, C.; Moro-oka, Y.; Hashimoto, S.; Kitagawa, T.; Toriumi, K.; Tatsumi, K.; Nakamura, A. *J. Am. Chem. Soc.* **1992**, *114*, 1277–1291. (d) Collins, M. A.; Feng, S. G.; White, P. A.; Templeton, J. L. *J. Am. Chem. Soc.* **1992**, *114*, 3771–3775. (e) Rowley, N. M.; Kurek, S. S.; George, M. W.; Hubig, S. M.; Beer, P. D.; Jones, C. J.; Kelly, J. M.; McCleverty, J. A. *J. Chem. Soc., Chem. Commun.* **1992**, 497–499. (f) Trofimenko, S.; Calabrese, J. C.; Thompson, J. S. *Inorg. Chem.* **1992**, *31*, 974–979. (g) Mohan, M.; Holmes, S. M.; Butcher, R. J.; Jasinski, J. P.; Carrano, C. J. *Inorg. Chem.* **1992**, *31*, 2029–2034.

(4) (a) Jezorek, J. R.; McCurdy, W. H., Jr. *Inorg. Chem.* **1975**, *14*, 1939–1944. (b) Yasuda, N.; Kokusen, H.; Sohrin, Y.; Kihara, S.; Matsui, M. *Bull. Chem. Soc. Jpn.* **1992**, *65*, 781–785.

(5) (a) Cowley, A. H.; Geerts, R. L.; Nunn, C. M.; Carrano, C. J. *J. Organomet. Chem.* **1988**, *341*, C27–C30. (b) Reger, D. L.; Knox, S. J.; Huff, M. F.; Rheingold, A. L.; Haggerty, B. S. *Inorg. Chem.* **1991**, *30*, 1754–1759. (c) Reger, D. L.; Huff, M. F.; Rheingold, A. L.; Haggerty, B. S. *J. Am. Chem. Soc.* **1992**, *114*, 579–584.

(6) (a) Restivo, R. J.; Ferguson, G.; O'Sullivan, D. J.; Lalor, F. J. *Inorg. Chem.* **1975**, *14*, 3046–3052. (b) De Gil, E. R.; Rivera, A. V.; Noguera, H. *Acta Crystallogr., Sect. B* **1977**, *33*, 2653–2655. (c) Cocivera, M.; Desmond, T. J.; Ferguson, G.; Kaitner, B.; Lalor, F. J.; O'Sullivan, D. J. *Organometallics* **1982**, *1*, 1125–1132. (d) Cocivera, M.; Ferguson, G.; Kaitner, B.; Lalor, F. J.; O'Sullivan, D. J.; Parvez, M.; Ruhl, B. *Organometallics* **1982**, *1*, 1132–1139.

(7) Holt, E. M.; Holt, S. L. *J. Chem. Soc., Dalton Trans.* **1973**, 1893–1896.

(8) Sohrin, Y.; Kokusen, H.; Kihara, S.; Matsui, M.; Kushi, Y.; Shiro, M. *Chem. Lett.* **1992**, 1461–1464.

0002-7863/93/1515-4128$04.00/0

Table I. Crystallographic Data for $[HB(pz)_3]_2Mg$ (**1**), $[HB(pz)_3]_2Ca$ (**2**), $[B(pz)_4]_2Mg$ (**3**), $[B(pz)_4]_2Be$ (**4**), and $[(HB(pz)_3)BeOH]_3$ (**5**)

	1	**2**	**3**	**4**	**5**
formula	$C_{18}H_{20}N_{12}B_2Mg$	$C_{18}H_{20}N_{12}B_2Ca$	$C_{24}H_{24}N_{16}B_2Mg$	$C_{24}H_{24}N_{16}B_2Be$	$C_{27}H_{33}N_{18}O_3B_3Be_3$
formula wt	450.36	466.14	582.49	567.19	717.14
cryst syst	triclinic	monoclinic	triclinic	monoclinic	rhombohedral (hexagonal axes)
space group	$P\bar{1}$	$C2/c$	$P\bar{1}$	$P2_1/c$	$R\bar{3}$ (h)
a, Å	10.836(4)	19.424(3)	12.142(3)	21.813(6)	19.037(2)
b, Å	11.642(2)	13.707(4)	12.298(3)	16.556(7)	
c, Å	10.608(3)	19.446(2)	9.835(4)	26.267(5)	17.194(6)
α, deg	90.11(2)		95.14(2)		
β, deg	113.70(2)	110.68(1)	103.19(2)	112.82(1)	
γ, deg	108.87(2)		100.14(2)		
V, Å^3	1146.1(7)	4844(2)	1394.6(7)	8743(4)	5397(2)
Z	2	8	2	12	6
cryst size, mm	0.50 × 0.50 × 0.05	0.70 × 0.20 × 0.20	0.25 × 0.10 × 0.10	0.30 × 0.20 × 0.20	0.32 × 0.32 × 0.32
d_{calcd}, g cm^{-3}	1.305	1.278	1.387	1.293	1.324
μ(Cu Kα), cm^{-1}	9.16	24.78	9.21	6.57	7.03
rflns collected	3624	3905	4371	12 701	1951
indep rflns	3414	3776	4144	12 300	1788
indep rflns obsd	2222	2353	2659	5417	1352
R	0.060	0.058	0.041	0.078	0.045
R_w	0.076	0.073	0.053	0.100	0.072

the conformation and bite size are controlled by intraligand contact between pyrazolyl rings bonded to the central boron atom rather than steric demand of the chelate ring itself. We report here that the intraligand contact results in an anomalous change in complex stability of $[B(pz)_4]^-$ depending on the ion size and formation of quite different structures of beryllium complexes with $[HB(pz)_3]^-$ and $[B(pz)_4]^-$.

Experimental Section

General Procedure. $K[H_2B(pz)_2]$, $K[HB(pz)_3]$, and $K[B(pz)_4]$ were synthesized as already reported.[9] All other chemicals were reagent-grade, and distilled water was used throughout. Acid dissociation constants of the protonated poly(pyrazolyl)borates were determined by potentiometric titration. Twenty milliliters of an aqueous solution containing 2×10^{-2} M $K[H_2B(pz)_2]$, $K[HB(pz)_3]$, or $K[B(pz)_4]$ was titrated with 0.1 M hydrochloric acid under a nitrogen atmosphere at 25.0 ± 0.1 °C. Metal ion and boron concentrations were determined with a Japan Jarrel Ash ICAP-500 inductively coupled argon plasma emission spectrometer. Proton NMR spectra were obtained at 25 ± 1 °C with a Varian VXR 200 spectrometer. Chemical shifts are reported (ppm) downfield from TMS using the solvent $CDCl_3$ (δ_H = 7.24) as an internal standard. The reported ^1H coupling constants are $^3J_{HH}$ values.

Extraction of Group 2 Metal Ions. An aliquot of chloroform (10 mL) was shaken with the equal volume of an aqueous phase containing 1×10^{-2} M $K[H_2B(pz)_2]$, $K[HB(pz)_3]$, or $K[B(pz)_4]$ and a group 2 metal ion (1×10^{-4} M) at 25 ± 1 °C. For aqueous solutions of pH 3–10, 1×10^{-2} M phthalic acid, acetic acid, 2-morpholinoethanesulfonic acid (MES), 3-morpholino-1-propanesulfonic acid (MOPS), 3-[(tris(hydroxymethyl)methyl)amino]-1-propanesulfonic acid (TAPS), or 2-(cyclohexylamino)ethanesulfonic acid (CHES) was added as a buffer. After the two phases were separated centrifugally, the pH of the aqueous phase was measured. The metal concentration in the aqueous phase was determined using the ICAP-500. The concentration in the organic phase was measured after back-extraction into 1 M nitric acid.

Bis[hydrotris(pyrazolyl)borato]magnesium, $[HB(pz)_3]_2Mg$ (1). Fifty milliliters of an aqueous solution of $K[HB(pz)_3]$ (5.0 g, 20 mmol) was added to an acidic aqueous solution (50 mL) of $MgCl_2 \cdot 6H_2O$ (2.0 g, 9.8 mmol). Sodium hydroxide solution (1 M) was added with mixing until the white precipitate no longer formed (pH 7). The white precipitate was filtered off, washed with distilled water and methanol, and purified by repeated recrystallization from chloroform. Crystals for the analytical sample and the X-ray structure were obtained by sublimation at 160 °C under 10^{-2} atm. Anal. Calcd for $C_{18}H_{20}N_{12}B_2Mg$: C, 48.01; H, 4.48; N, 37.32; B, 4.80; Mg, 5.40. Found: C, 47.73; H, 4.43; N, 37.34; B, 4.89; Mg, 5.24. mp: 278–279 °C. ^1H NMR ($CDCl_3$, δ): 6.06 (6, t, J = 2.0 Hz, 4-H (pz)), 7.15, 7.70 (6, 6, d, d, J = 1.8 Hz, 3-H, 5-H (pz)).

Bis[hydrotris(pyrazolyl)borato]calcium, $[HB(pz)_3]_2Ca$ (2). Fifty milliliters of an aqueous solution of $K[HB(pz)_3]$ (6.1 g, 24 mmol) was added to an acidic aqueous solution (15 mL) of $CaCl_2 \cdot 2H_2O$ (1.7 g, 12 mmol). Sodium hydroxide solution (1 M) was added with mixing until the white precipitate no longer formed (pH 9). The white precipitate was filtered off, washed with distilled water and methanol, and purified by repeated recrystallization from toluene. Crystals for the analytical sample and the X-ray structure were obtained by sublimation at 160 °C under 10^{-2} atm. Anal. Calcd for $C_{18}H_{20}N_{12}B_2Ca$: C, 46.38; H, 4.32; N, 36.06; B, 4.64; Ca, 8.60. Found: C, 46.14; H, 4.27; N, 35.95; B, 4.57; Ca, 8.36. mp: 275–276 °C. ^1H NMR ($CDCl_3$, δ): 6.15 (6, t, J = 1.9 Hz; 4-H (pz)), 7.51, 7.75 (6, 6, d, d, J = 1.8, 2.2 Hz, 3-H, 5-H (pz)).

Bis[tetrakis(pyrazolyl)borato]magnesium, $[B(pz)_4]_2Mg$ (3). Compound **3** was extracted into 40 mL of dichloromethane from a 200-mL aqueous solution of pH 8 containing 0.050 M $MgCl_2$ and 0.11 M $K[B(pz)_4]$. Crystals for the analytical sample and the X-ray structure were grown from dichloromethane. Anal. Calcd for $C_{24}H_{24}N_{16}B_2Mg$: C, 49.49; H, 4.15; N, 38.47; B, 3.71; Mg, 4.17. Found: C, 48.90; H, 4.14; N, 38.23; B, 3.71; Mg, 4.13. mp: 353–354 °C. ^1H NMR ($CDCl_3$, δ): 6.09, 6.63 (6, 2, t, br, J = 2.0 Hz, 4-H (pz)), 7.20, 7.68, 8.00, 8.17 (6, 6, 2, 2, d, d, br, d, J = 1.6, 2.2, 1.6 Hz, 3-H, 5-H (pz)).

Bis[tetrakis(pyrazolyl)borato]beryllium, $[B(pz)_4]_2Be$ (4). Compound **4** was extracted into 30 mL of dichloromethane from a 100-mL aqueous solution of pH 4.5 containing 0.020 M $BeCl_2$ and 0.044 M $K[B(pz)_4]$. Removal of the solvent afforded a white solid, which was purified by repeated recrystallization from benzene and sublimation of contaminating pyrazole at 100 °C, 10^{-2} atm. Recrystallization from a mixture of chloroform and hexane in a 1:2 volume ratio gave colorless crystals suitable for X-ray diffraction. Anal. Calcd for $C_{24}H_{24}N_{16}B_2Be$: C, 50.82; H, 4.27; N, 39.51; B, 3.81; Be, 1.59. Found: C, 49.47; H, 4.26; N, 38.47; B, 3.85; Be, 1.57. mp: 232–233 °C. ^1H NMR ($CDCl_3$, δ): 6.25, 6.26, (4, 4, t, t, J = 2.0, 2.2 Hz, 4-H (pz)), 6.62, 6.69, 7.35, 7.77 (4, 4, 4, 4, all d, J = 2.2, 2.6, 2.0, 1.2 Hz, 3-H, 5-H (pz)).

Tris[hydrotris(pyrazolyl)borato]tri-μ-hydroxytri*cyclo*beryllium, $[(HB(pz)_3)BeOH]_3$ (5). Extraction of **5** into 30 mL of dichloroethane from 100 mL of an aqueous solution of pH 5.0 containing 0.020 M $BeCl_2$ and 0.022 M $K[HB(pz)_3]$ followed by removal of solvent yielded a pink-tinged white solid. Analytically pure **5** was obtained by repeated recrystallization from chloroform. The colorless crystals suitable for X-ray diffraction were afforded by recrystallization from a mixture of chloroform and hexane in a 1:2 volume ratio. Anal. Calcd for $C_{27}H_{33}N_{18}O_3B_3Be_3$: C, 45.21; H, 4.65; N, 35.16; B, 4.52; Be, 3.77. Found: C, 44.46; H, 4.78; N, 34.90; B, 4.77; Be, 3.83. mp: 188 °C dec. ^1H NMR ($CDCl_3$, δ): 6.00, 6.21 (3, 6, t, t, J = 1.9, 2.2 Hz, 4-H (pz)), 6.96, 7.60, 7.66, 7.68 (3, 6, 6, 3, all d, J = 1.6, 2.2, 1.8, 2.0 Hz, 3-H, 5-H (pz)), 7.72 (3, br, OH). IR: 2450 (s, ν_{B-H}), 3200 cm^{-1} (br, ν_{O-H}). MS: m/e 717 ($[(HB(pz)_3)BeOH]_3$).

X-ray Crystal Structure Determination. Crystallographic data are summarized in Table I. Colorless crystals of **1–5** were each mounted on fine glass fibers with epoxy cement. The lattice parameters and intensity data were measured on a Rigaku AFC5R diffractometer with graphite monochromated Cu Kα radiation (λ = 1.541 78 Å) at 23 ± 1 °C. The $\omega - 2\theta$ scan technique to a maximum 2θ value of 120° was used. An

(9) Trofimenko, S. *J. Am. Chem. Soc.* **1967**, *89*, 3170–3177.

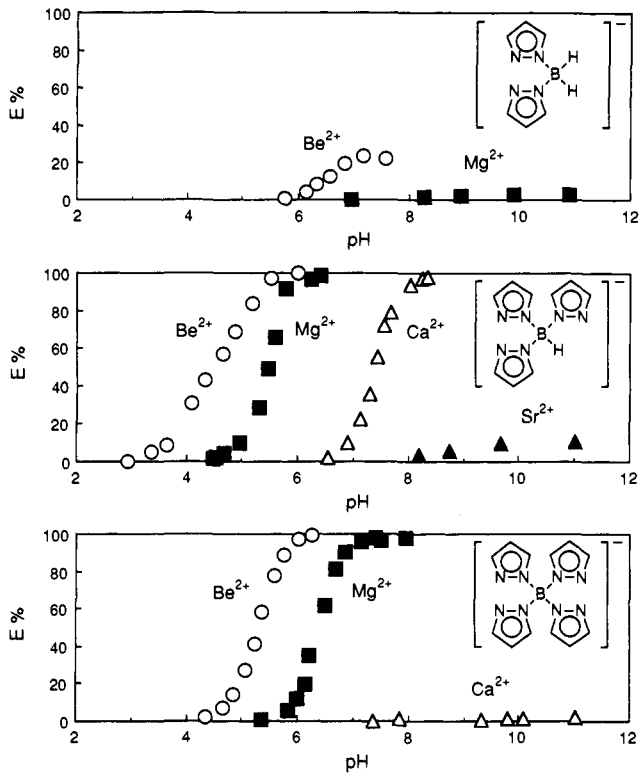

Figure 1. Effect of pH on the extraction of group 2 metal ions. Aqueous phase: 1×10^{-2} M $K[H_nB(pz)_{4-n}]$, 1×10^{-2} M buffer, 1×10^{-4} M M^{2+} (10 mL). Organic phase: chloroform (10 mL). Shaking: 5 min at 25 °C.

empirical absorption correction was applied to the data sets.[10] Structures **1–3** were solved by a combination of the Patterson method[11] and a direct method,[12] and those of **4** and **5** were solved by direct methods.[12,13] The non-hydrogen atoms, except for those of **4**, were refined anisotropically. For the complex **4**, the isotropic temperature factors were used for the nitrogen and carbon atoms of the noncoordinated pyrazolyl groups because of the small reflection/parameter ratio when the anisotropic factors were used for all atoms.

Figures 2–6 show the ORTEP drawings of **1–5**, respectively. For **1–4**, only one of the independent molecules is shown. Tables II–VI contain selected bond distances and bond angles for **1–5**, respectively.

Results

Acid Dissociation Constants of the Protonated Poly(pyrazolyl)borates. Dihydrobis(pyrazolyl)borate is protonated as shown in Scheme I.

Scheme I

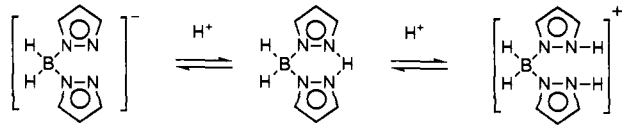

The acid dissociation constants of the protonated ligands are defined as

$$K_{a1} = [H^+][A^-]/[HA] \quad (1)$$

$$K_{a2} = [H^+][HA]/[H_2A^+] \quad (2)$$

where brackets represent the molar concentration in aqueous solution and A^- stands for a poly(pyrazolyl)borate anion. For $[H_2B(pz)_2]^-$, pK_{a1} and pK_{a2} were found to be 8.70 ± 0.03 and 4.99 ± 0.06, respectively.[4b] These values are much higher than the pK_a of pyrazole (2.60).[14] Although $[HB(pz)_3]^-$ and $[B(pz)_4]^-$ can combine with a maximum of three or four protons, only pK_{a1} values were determined. The pK_{a1} is 6.92 ± 0.03 for $[HB(pz)_3]^-$ and 6.06 ± 0.04 for $[B(pz)_4]^-$.

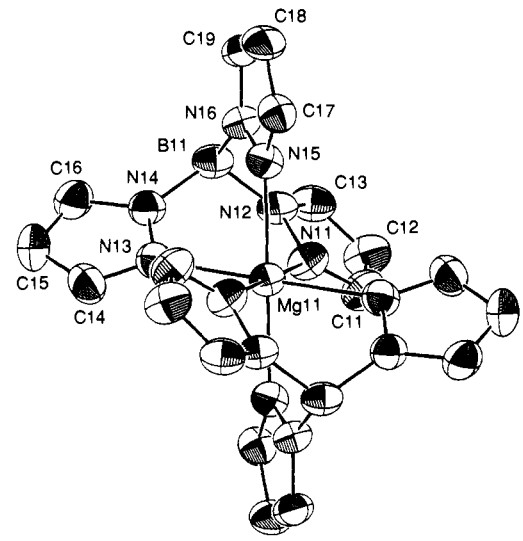

Figure 2. ORTEP view of one of the independent molecules of $[HB(pz)_3]_2Mg$ (**1**) (50% probability). Hydrogen atoms are omitted for clarity.

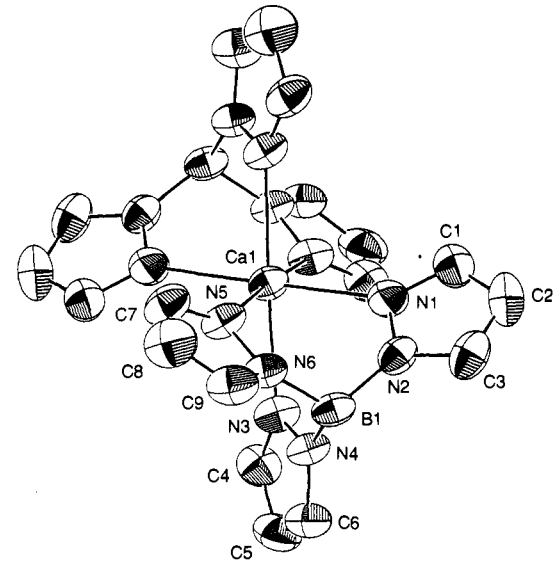

Figure 3. ORTEP view of one of the independent molecules of $[HB(pz)_3]_2Ca$ (**2**) (50% probability). Hydrogen atoms are omitted for clarity.

Extraction of Group 2 Metal Ions. Figure 1 shows the relationship between the extracted percentage of a metal ion (E %) and pH of the aqueous phase. The initial concentrations of $K[H_nB(pz)_{4-n}]$ and the metal ion are 1×10^{-2} and 1×10^{-4} M, respectively. With $[H_2B(pz)_2]^-$, maximum E % is 24% for Be^{2+} and 3% for Mg^{2+}. Significant extraction of Ca^{2+}, Sr^{2+}, and Ba^{2+} does not occur. With $[HB(pz)_3]^-$, Be^{2+}, Mg^{2+}, and Ca^{2+} are extracted quantitatively, and Sr^{2+} is extracted up to 11%. With $[B(pz)_4]^-$, although Be^{2+} and Mg^{2+} are extracted quantitatively, only 2% of Ca^{2+} is extracted. These data were obtained after 5 min of shaking. The E % was not dependent on the shaking time

(10) Walker, N.; Stuart, D. *Acta Crystallogr., Sect. A* **1983**, *39*, 158–166.
(11) Calbrese, J. C. Ph.D. Thesis, Univ. of Wisconsin-Madison, 1972.
(12) Beurskens, P. T. Technical Report 1984/1 Crystallography Laboratory: Toernooiveld, 6525 Ed Nijmegen, the Netherlands, 1984.
(13) Gilmore, C. J. *J. Appl. Crystallogr.* **1984**, *17*, 42–46.
(14) Perrin, D. D. *Stability Constants of Metal-Ion Complexes, Part B, Organic Ligands*; IUPAC Chemical Data Series 22; Pergamon Press: Oxford, 1979; p 103.

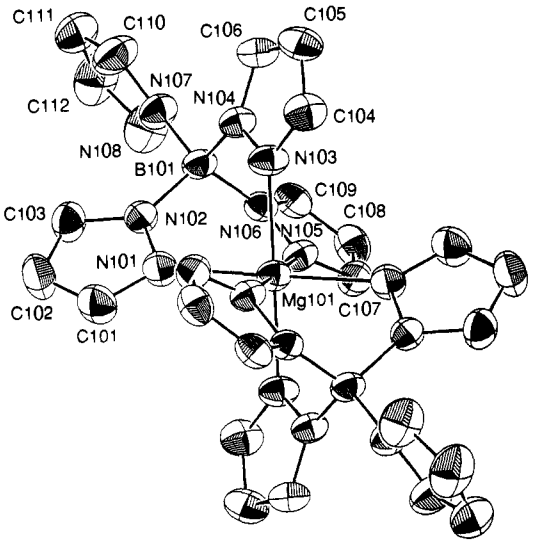

Figure 4. ORTEP view of one of the independent molecules of $[B(pz)_4]_2Mg$ (**3**) (50% probability). Hydrogen atoms are omitted for clarity.

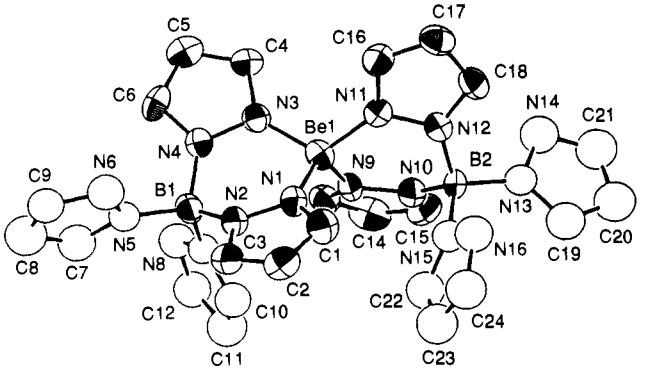

Figure 5. ORTEP view of one of the independent molecules of $[B(pz)_4]_2Be$ (**4**) (50% probability). Hydrogen atoms are omitted for clarity.

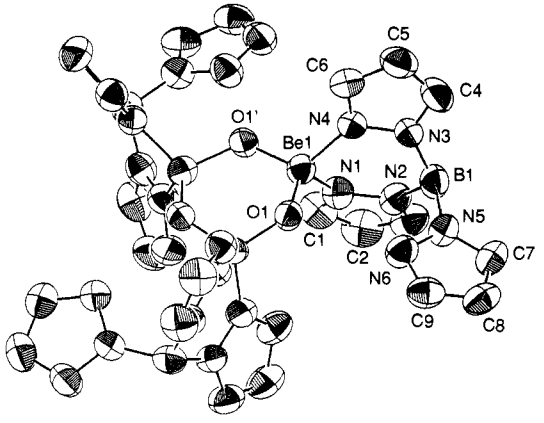

Figure 6. ORTEP view of $[(HB(pz)_3)BeOH]_3$ (**5**) (50% probability). Hydrogen atoms are omitted for clarity.

of 1–5 min except for the extraction of Be^{2+} with $[B(pz)_4]^-$. When the shaking time was prolonged beyond 5 min, the E % generally decreased. This is because poly(pyrazolyl)borate ligands decompose to pyrazole and boric acid in aqueous solution. The decomposition of ligands was ascertained by ^1H NMR measurement in D_2O. The E % of Be^{2+} with $[B(pz)_4]^-$ increased with increasing shaking time and reached a maximum after 3 h. As an example, the E % at pH 4.90 rose from 16.6% to 92.6% when the shaking time was prolonged from 5 min to 3 h. The complex formation of Be^{2+} with $[B(pz)_4]^-$ is probably a slow reaction.

Table II. Selected Bond Distances (Å) and Bond Angles (deg) for $[HB(pz)_3]_2Mg$ (**1**)

Molecule 1			
Bond Distances			
Mg(1)–N(1)	2.149(4)	Mg(1)–N(3)	2.190(4)
Mg(1)–N(5)	2.214(4)	N(1)–N(2)	1.365(5)
N(2)–B(1)	1.541(7)	N(3)–N(4)	1.370(5)
N(4)–B(1)	1.529(7)	N(5)–N(6)	1.359(5)
N(6)–B(1)	1.545(7)		
Bond Angles			
N(1)–Mg(1)–N(1′)	180.00	N(1)–Mg(1)–N(3)	86.0(1)
N(1)–Mg(1)–N(5)	85.8(1)	N(3)–Mg(1)–N(3′)	180.00
N(3)–Mg(1)–N(5)	81.7(1)	N(5)–Mg(1)–N(5′)	180.00
Mg(1)–N(1)–N(2)	119.0(3)	N(1)–N(2)–B(1)	120.5(3)
Mg(1)–N(3)–N(4)	118.2(3)	N(3)–N(4)–B(1)	120.3(3)
Mg(1)–N(5)–N(6)	118.3(3)	N(5)–N(6)–B(1)	119.6(3)
N(2)–B(1)–N(4)	110.0(4)	N(2)–B(1)–N(6)	108.9(4)
N(4)–B(1)–N(6)	108.8(4)		
Molecule 2			
Bond Distances			
Mg(11)–N(11)	2.149(3)	Mg(11)–N(13)	2.199(4)
Mg(11)–N(15)	2.206(4)	N(11)–N(12)	1.359(5)
N(12)–B(11)	1.539(6)	N(13)–N(14)	1.364(5)
N(14)–B(11)	1.537(6)	N(15)–N(16)	1.365(4)
N(16)–B(11)	1.544(6)		
Bond Angles			
N(11)–Mg(11)–N(11′)	180.00	N(11)–Mg(11)–N(13)	86.6(1)
N(11)–Mg(11)–N(15)	85.9(1)	N(13)–Mg(11)–N(13′)	180.00
N(13)–Mg(11)–N(15)	81.9(1)	N(15)–Mg(11)–N(15′)	180.00
Mg(11)–N(11)–N(12)	119.1(2)	N(11)–N(12)–B(11)	120.9(3)
Mg(11)–N(13)–N(14)	117.5(3)	N(13)–N(14)–B(11)	121.3(3)
Mg(11)–N(15)–N(16)	117.1(3)	N(15)–N(16)–B(11)	121.4(3)
N(12)–B(11)–N(14)	110.5(4)	N(12)–B(11)–N(16)	108.6(4)
N(14)–B(11)–N(16)	106.8(3)		

Syntheses of Complexes. Complexes with two $[HB(pz)_3]^-$ coordinated to Mg^{2+} and Ca^{2+} and with two $[B(pz)_4]^-$ coordinated to Be^{2+} and Mg^{2+} were prepared by addition of aqueous sodium hydroxide to the acidic aqueous solution containing MCl_2 and 2 equiv of the ligand (eq 3). These complexes were obtained as

$$M^{2+} + 2H[H_nB(pz)_{4-n}] \rightleftharpoons [H_nB(pz)_{4-n}]_2M + 2H^+ \quad (3)$$

precipitates and extracted into chloroform, dichloromethane, and benzene.

Extracted species of Be^{2+} with $[HB(pz)_3]^-$ were changed depending upon the initial concentration of Be^{2+} in the aqueous phase ($[Be^{2+}]_i$), even if a sufficient quantity of the ligand was present to form $[HB(pz)_3]_2Be$. When $[Be^{2+}]_i$ was 1×10^{-2} M or above, the mole ratio of Be:B of the extracted species was 1:1. The ratio approached 1:2 as $[Be^{2+}]_i$ decreased. The 1:1 species was successfully isolated and proved to be $[(HB(pz)_3)BeOH]_3$.

Both the Be^{2+} complexes of $[B(pz)_4]^-$ and $[HB(pz)_3]^-$ were readily hydrolyzed in alkaline aqueous solution. Maintaining the pH below 6 was necessary to obtain the complexes.

All five complexes were stable in air for over a year.

Structure of $[HB(pz)_3]_2Mg$ (1). Two crystallographically independent molecules, lying on an inversion point in the crystal, respectively, are contained in a unit cell of complex **1**. These two molecules resemble each other. Figure 2 shows an ORTEP drawing of one of these molecules; Table II shows selected bond distances and angles. The molecule is monomeric with no short intermolecular contacts. The magnesium atom sits on a center of inversion. Both ligands are tridentate, and the geometry about the magnesium atom is a trigonally distorted octahedron. This structure is similar to the structure observed for [HB(3,5-

Table III. Selected Bond Distances (Å) and Bond Angles (deg) for $[HB(pz)_3]_2Ca$ (**2**)

Molecule 1

Bond Distances

Ca(1)–N(1)	2.407(4)	Ca(1)–N(3)	2.449(4)
Ca(1)–N(5)	2.447(4)	N(1)–N(2)	1.366(5)
N(2)–B(1)	1.551(7)	N(3)–N(4)	1.354(5)
N(4)–B(1)	1.534(6)	N(5)–N(6)	1.364(5)
N(6)–B(1)	1.543(6)		

Bond Angles

N(1)–Ca(1)–N(1′)	179.1(2)	N(1)–Ca(1)–N(3)	80.6(1)
N(1)–Ca(1)–N(5)	80.7(1)	N(3)–Ca(1)–N(3′)	98.4(2)
N(3)–Ca(1)–N(5)	76.5(1)	N(5)–Ca(1)–N(5′)	108.6(2)
Ca(1)–N(1)–N(2)	119.3(3)	N(1)–N(2)–B(1)	122.1(3)
Ca(1)–N(3)–N(4)	118.4(3)	N(3)–N(4)–B(1)	122.7(3)
Ca(1)–N(5)–N(6)	117.3(3)	N(5)–N(6)–B(1)	123.4(3)
N(2)–B(1)–N(4)	110.7(4)	N(2)–B(1)–N(6)	110.5(4)
N(4)–B(1)–N(6)	109.6(4)		

Molecule 2

Bond Distances

Ca(2)–N(7)	2.460(4)	Ca(2)–N(9)	2.458(4)
Ca(2)–N(11)	2.425(4)	N(7)–N(8)	1.359(5)
N(8)–B(2)	1.535(7)	N(9)–N(10)	1.361(5)
N(10)–B(2)	1.539(7)	N(11)–N(12)	1.352(5)
N(12)–B(2)	1.546(7)		

Bond Angles

N(7)–Ca(2)–N(7′)	105.0(2)	N(7)–Ca(2)–N(9)	76.0(1)
N(7)–Ca(2)–N(11)	80.6(1)	N(9)–Ca(2)–N(9′)	103.0(2)
N(9)–Ca(2)–N(11)	80.7(1)	N(11)–Ca(2)–N(11′)	179.1(2)
Ca(2)–N(7)–N(8)	118.0(3)	N(7)–N(8)–B(2)	122.6(3)
Ca(2)–N(9)–N(10)	117.7(3)	N(9)–N(10)–B(2)	123.0(3)
Ca(2)–N(11)–N(12)	118.5(3)	N(11)–N(12)–B(2)	123.2(3)
N(8)–B(2)–N(10)	109.6(4)	N(8)–B(2)–N(12)	110.9(4)
N(10)–B(2)–N(12)	110.7(4)		

$Me_2pz)_3]_2Mg$, and the average Mg–N bond distances of these molecules are identical (2.19(3) Å).[15]

Structure of $[HB(pz)_3]_2Ca$ (2). A unit cell of complex **2** also contains two similar but crystallographically independent molecules, the two calcium atoms lying on different inversion points in the crystal. Figure 3 shows an ORTEP drawing of one of these molecules; Table III shows selected bond distances and angles. Similarly to **1**, both ligands are tridentate, and the geometry about the calcium atom is a trigonally distorted octahedron. The planes formed by the three nitrogen donor atoms of each ligand are parallel. The Ca–N bond distance (2.44(2) Å) is longer than the Mg–N distance, and the intraligand N–Ca–N bond angle (79.2(2.1)°) is smaller than the N–Mg–N angle (84.7(2.0)°). Examination of the edge lengths of the octahedron formed by donor atoms reveals that the trigonal distortion of **2** is more enhanced than the distortion of **1**. The mean interligand N···N distance is 9.8% and 20.9% longer than the mean intraligand N···N distance (bite size) for **1** and **2**, respectively.

Structure of $[B(pz)_4]_2Mg$ (3). A unit cell of complex **3** also contains two crystallographically independent molecules, of which the magnesium atoms lie on inversion points in the crystal. Figure 4 shows an ORTEP drawing of one of these molecules; Table IV shows selected bond distances and angles. Similarly to **1**, the magnesium atom sits on a center of inversion. Both ligands are tridentate, forming a six-coordinated, monomeric structure. The noncoordinated pyrazolyl ring stands out in the direction opposite the metal atom. The other molecule in the unit cell has the same structure as that shown in Figure 4 except that the axial and noncoordinated pyrazolyl rings incline in the opposite direction of those shown in Figure 4. The bond distances and angles of the bidentate pyrazolyls do not present any significant difference

(15) Han, R.; Parkin, G. *J. Organomet. Chem.* **1990**, *393*, C43–C46.

Table IV. Selected Bond Distances (Å) and Bond Angles (deg) for $[B(pz)_4]_2Mg$ (**3**)

Molecule 1

Bond Distances

Mg(1)–N(1)	2.202(3)	Mg(1)–N(3)	2.158(3)
Mg(1)–N(5)	2.108(3)	N(1)–N(2)	1.370(4)
N(2)–B(1)	1.549(5)	N(3)–N(4)	1.362(4)
N(4)–B(1)	1.560(4)	N(5)–N(6)	1.362(4)
N(6)–B(1)	1.552(5)	N(7)–N(8)	1.369(4)
N(7)–B(1)	1.518(5)		

Bond Angles

N(1)–Mg(1)–N(1′)	180.00	N(1)–Mg(1)–N(3)	83.0(1)
N(1)–Mg(1)–N(5)	84.8(1)	N(3)–Mg(1)–N(3′)	180.00
N(3)–Mg(1)–N(5)	86.2(1)	N(5)–Mg(1)–N(5′)	180.00
Mg(1)–N(1)–N(2)	118.9(2)	N(1)–N(2)–B(1)	118.5(3)
Mg(1)–N(3)–N(4)	121.5(2)	N(3)–N(4)–B(1)	117.2(2)
Mg(1)–N(5)–N(6)	118.3(2)	N(5)–N(6)–B(1)	122.2(3)
N(8)–N(7)–B(1)	120.2(3)	N(2)–B(1)–N(4)	106.5(3)
N(2)–B(1)–N(6)	109.7(3)	N(2)–B(1)–N(7)	110.7(3)
N(4)–B(1)–N(6)	109.9(3)	N(4)–B(1)–N(7)	112.3(3)
N(6)–B(1)–N(7)	107.8(3)		

Molecule 2

Bond Distances

Mg(101)–N(101)	2.143(3)	Mg(101)–N(103)	2.172(3)
Mg(101)–N(105)	2.167(3)	N(101)–N(102)	1.363(4)
N(102)–B(101)	1.562(5)	N(103)–N(104)	1.368(4)
N(104)–B(101)	1.551(5)	N(105)–N(106)	1.376(4)
N(106)–B(101)	1.544(5)	N(107)–N(108)	1.359(4)
N(107)–B(101)	1.512(5)		

Bond Angles

N(101)–Mg(101)–N(101′)	180.00	N(101)–Mg(101)–N(103)	85.1(1)
N(101)–Mg(101)–N(105)	85.5(1)	N(103)–Mg(101)–N(103′)	180.00
N(103)–Mg(101)–N(105)	83.7(1)	N(105)–Mg(101)–N(105′)	180.00
Mg(101)–N(101)–N(102)	117.8(2)	N(101)–N(102)–B(101)	122.1(3)
Mg(101)–N(103)–N(104)	119.1(2)	N(103)–N(104)–B(101)	119.6(3)
Mg(101)–N(105)–N(106)	121.3(2)	N(105)–N(106)–B(101)	117.2(3)
N(108)–N(107)–B(101)	120.4(3)	N(102)–B(101)–N(104)	109.6(3)
N(102)–B(101)–N(106)	109.2(3)	N(102)–B(101)–N(107)	107.4(3)
N(104)–B(101)–N(106)	107.3(3)	N(104)–B(101)–N(107)	109.6(3)
N(106)–B(101)–N(107)	113.7(3)		

from those of the monodentate. Both the interligand and intraligand N···N distances of **3** are nearly equal to the distances of **1**.

Structure of $[B(pz)_4]_2Be$ (4). There are three crystallographically independent molecules within a unit cell. These molecules are similar to one another in structure. Figure 5 shows an ORTEP drawing of one of these molecules; Table V shows selected bond distances and angles. The molecule is monomeric with no short intermolecular contacts. Each ligand is coordinated to the beryllium atom in a bidentate fashion. The noncoordinated ring farthest from the metal is oriented so as to bisect the planes of the two coordinated rings. The fourth ring is oriented perpendicular to the distant noncoordinated ring. Complex **4** is a rare example of beryllium complexes which are formed in aqueous solution and contain the tetrahedral beryllium atom coordinated with four nitrogen atoms.[16] The average Be–N distance is 1.70(2) Å, which is shorter than the Be–N distance (1.73–1.77 Å) about the tetrahedral beryllium atoms in $Be(NH_2)_2$[17] or that (1.78–1.81 Å) in $[HB(3\text{-}Bu^tpz)_3]BeX$ (X = H, Br) where the poly(pyrazolyl)borate is tridentate.[18]

Structure of $[(HB(pz)_3)BeOH]_3$ (5). Complex **5** lies on a 3-fold axis in the crystal. Figure 6 shows an ORTEP drawing of **5**; Table VI shows selected bond distances and angles. The structure of **5** consists of a cyclic $[BeOH]_3^{3+}$ moiety and has C_3 symmetry. The $[BeOH]_3^{3+}$ is the dominant species of beryllium in aqueous

(16) Cotton, F. A.; Wilkinson, G. *Advanced Inorganic Chemistry*, 4th ed.; John Wiley & Sons: New York, 1980.
(17) Jacobs, V. H. *Z. Anorg. Allg. Chem.* **1976**, *427*, 1–7.
(18) Han, R.; Parkin, G. *Inorg. Chem.* **1992**, *31*, 983–988.

Table V. Selected Bond Distances (Å) and Bond Angles (deg) for $[B(pz)_4]_2Be$ (**4**)

Molecule 1

Bond Distances

N(1)–N(2)	1.368(7)	N(1)–Be(1)	1.72(1)	N(9)–N(10)	1.359(7)	N(9)–Be(1)	1.72(1)
N(2)–B(1)	1.52(1)	N(3)–N(4)	1.369(6)	N(10)–B(2)	1.52(1)	N(11)–N(12)	1.368(7)
N(3)–Be(1)	1.68(1)	N(4)–B(1)	1.563(9)	N(11)–Be(1)	1.68(1)	N(12)–B(2)	1.55(1)
N(5)–N(6)	1.371(8)	N(5)–B(1)	1.503(9)	N(13)–N(14)	1.369(7)	N(13)–B(2)	1.501(9)
N(7)–N(8)	1.377(8)	N(7)–B(1)	1.53(1)	N(15)–N(16)	1.378(8)	N(15)–B(2)	1.534(9)

Bond Angles

N(2)–N(1)–Be(1)	121.6(5)	N(1)–N(2)–B(1)	122.4(5)	N(4)–B(1)–N(7)	111.1(6)	N(5)–B(1)–N(7)	111.4(6)
N(4)–N(3)–Be(1)	121.5(5)	N(3)–N(4)–B(1)	122.5(5)	N(10)–B(2)–N(12)	109.0(6)	N(10)–B(2)–N(13)	110.2(6)
N(6)–N(5)–B(1)	120.6(6)	N(8)–N(7)–B(1)	121.0(6)	N(10)–B(2)–N(15)	108.9(5)	N(12)–B(2)–N(13)	109.7(5)
N(10)–N(9)–Be(1)	121.5(5)	N(9)–N(10)–B(2)	121.0(5)	N(12)–B(2)–N(15)	110.1(6)	N(13)–B(2)–N(15)	109.0(6)
N(12)–N(11)–Be(1)	122.7(5)	N(11)–N(12)–B(2)	120.4(5)	N(1)–Be(1)–N(3)	102.9(5)	N(1)–Be(1)–N(9)	115.7(6)
N(14)–N(13)–B(2)	120.4(6)	N(16)–N(15)–B(2)	120.3(6)	N(1)–Be(1)–N(11)	111.3(6)	N(3)–Be(1)–N(9)	108.9(6)
N(2)–B(1)–N(4)	107.6(5)	N(2)–B(1)–N(5)	110.1(6)	N(3)–Be(1)–N(11)	115.7(6)	N(9)–Be(1)–N(11)	102.7(5)
N(2)–B(1)–N(7)	107.8(6)	N(4)–B(1)–N(5)	108.8(6)				

Molecule 2

Bond Distances

N(101)–N(102)	1.365(7)	N(101)–Be(11)	1.70(1)	N(109)–N(110)	1.368(7)	N(109)–Be(11)	1.72(1)
N(102)–B(101)	1.53(1)	N(103)–N(104)	1.365(7)	N(110)–B(102)	1.53(1)	N(111)–N(112)	1.378(7)
N(103)–Be(11)	1.71(1)	N(104)–B(101)	1.541(9)	N(111)–Be(11)	1.67(1)	N(112)–B(102)	1.542(9)
N(105)–N(106)	1.366(8)	N(105)–B(101)	1.52(1)	N(113)–N(114)	1.364(8)	N(113)–B(102)	1.53(1)
N(107)–N(108)	1.380(8)	N(107)–B(101)	1.504(9)	N(115)–N(116)	1.368(8)	N(115)–B(102)	1.52(1)

Bond Angles

N(102)–N(101)–Be(11)	123.2(5)	N(101)–N(102)–B(101)	120.1(5)	N(104)–B(101)–N(107)	111.2(6)	N(105)–B(101)–N(107)	110.6(6)
N(104)–N(103)–Be(11)	121.2(5)	N(103)–N(104)–B(101)	122.1(5)	N(110)–B(102)–N(112)	108.5(6)	N(110)–B(102)–N(113)	109.6(6)
N(106)–N(105)–B(101)	119.5(6)	N(108)–N(107)–B(101)	119.5(6)	N(110)–B(102)–N(115)	109.5(6)	N(112)–B(102)–N(113)	107.9(6)
N(110)–N(109)–Be(11)	119.9(5)	N(109)–N(110)–B(102)	121.6(5)	N(112)–B(102)–N(115)	110.7(6)	N(113)–B(102)–N(115)	110.7(6)
N(112)–N(111)–Be(11)	120.8(5)	N(111)–N(112)–B(102)	122.2(5)	N(101)–Be(11)–N(103)	102.7(5)	N(101)–Be(11)–N(109)	117.8(6)
N(114)–N(113)–B(102)	119.9(6)	N(116)–N(115)–B(102)	119.2(6)	N(101)–Be(11)–N(111)	110.7(6)	N(103)–Be(11)–N(109)	108.3(6)
N(102)–B(101)–N(104)	108.8(5)	N(102)–B(101)–N(105)	109.5(6)	N(103)–Be(11)–N(111)	113.5(6)	N(109)–Be(11)–N(111)	104.2(5)
N(102)–B(101)–N(107)	109.4(6)	N(104)–B(101)–N(105)	107.3(6)				

Molecule 3

Bond Distances

N(201)–N(202)	1.366(6)	N(201)–Be(21)	1.71(1)	N(209)–N(210)	1.370(7)	N(209)–Be(21)	1.71(1)
N(202)–B(201)	1.528(8)	N(203)–N(204)	1.361(6)	N(210)–B(202)	1.56(1)	N(211)–N(212)	1.368(7)
N(203)–Be(21)	1.70(1)	N(204)–B(201)	1.531(9)	N(211)–Be(21)	1.70(1)	N(212)–B(202)	1.52(1)
N(205)–N(206)	1.376(8)	N(205)–B(201)	1.508(9)	N(213)–N(214)	1.364(9)	N(213)–B(202)	1.52(1)
N(207)–N(208)	1.386(8)	N(207)–B(201)	1.513(9)	N(215)–N(216)	1.379(8)	N(215)–B(202)	1.51(1)

Bond Angles

N(202)–N(201)–Be(21)	121.7(5)	N(201)–N(202)–B(201)	122.2(5)	N(204)–B(201)–N(207)	110.1(6)	N(205)–B(201)–N(207)	110.2(5)
N(204)–N(203)–Be(21)	122.4(5)	N(203)–N(204)–B(201)	122.2(5)	N(210)–B(202)–N(212)	108.5(6)	N(210)–B(202)–N(213)	107.3(6)
N(206)–N(205)–B(201)	119.1(5)	N(208)–N(207)–B(201)	119.3(5)	N(210)–B(202)–N(215)	108.0(7)	N(212)–B(202)–N(213)	109.7(7)
N(210)–N(209)–Be(21)	121.5(5)	N(209)–N(210)–B(202)	120.8(6)	N(212)–B(202)–N(215)	111.7(7)	N(213)–B(202)–N(215)	111.6(7)
N(212)–N(211)–Be(21)	121.2(6)	N(211)–N(212)–B(202)	122.7(5)	N(201)–Be(21)–N(203)	102.7(6)	N(201)–Be(21)–N(209)	117.8(7)
N(214)–N(213)–B(202)	118.9(7)	N(216)–N(215)–B(202)	117.7(6)	N(201)–Be(21)–N(211)	108.1(6)	N(203)–Be(21)–N(209)	107.9(6)
N(202)–B(201)–N(204)	108.0(5)	N(202)–B(201)–N(205)	108.9(6)	N(203)–Be(21)–N(211)	117.1(7)	N(209)–Be(21)–N(211)	103.9(6)
N(202)–B(201)–N(207)	108.1(5)	N(204)–B(201)–N(205)	111.4(6)				

solution in the course of hydrolysis of Be^{2+}.[19] The cyclic structure of $[BeOH]_3^{3+}$ has been determined in $[(C_5H_4NCOO)BeOH]_3 \cdot H_2O$, where the ring has a shallow chair conformation.[20] Although the bond distances and angles of $[BeOH]_3^{3+}$ in **5** are similar to those in $[(C_5H_4NCOO)BeOH]_3 \cdot H_2O$, $[BeOH]_3^{3+}$ in **5** is more puckered. The $[HB(pz)_3]^-$ in **5** is bidentate, and the geometry about the beryllium atom is a distorted tetrahedron. With respect to the chelate ring in **5**, while the bite size (2.66(1) Å) is similiar to that of **4**, the Be–N distance (1.74(1) Å) is longer and the N–Be–N angle (99.5 (0.2)°) is smaller than those of **4**.

Another important result of the determination of the structure of **5** is that the existence of OH–N hydrogen bonding between the bridged hydroxide and noncoordinated pyrazolyl ring is shown by the following facts. The N5–N6 bond of the noncoordinated pyrazolyl ring is almost coplanar with the Be1–O1 bond (dihedral angle of N5–N6–O1–Be1 is 4.0°). The distance of O1–N6 is 2.85 Å, and the angles of O1–H–N6 and N5–N6–H are 168.4° and 122.4°, respectively. The IR spectrum shows a broad absorption of the hydroxide group at 3200 cm^{-1}.[21] In the ^1H NMR spectrum, the resonance of the hydroxide proton appears at 7.72 ppm, which is considerably shifted downfield.[22] Accordingly, each $[HB(pz)_3]^-$ is bound to the $[BeOH]_3^{3+}$ moiety by one OH–N hydrogen bond in addition to two Be–N bonds. Complex **5** is the demonstration for the first time that poly(pyrazolyl)borates can stabilize a molecule by multiple-point bindings.

(19) (a) Kakihana, H.; Sillén, L. G. *Acta Chem. Scand.* **1956**, *10*, 985–1005. (b) Ishiguro, S.; Maeda, M.; Ono, S.; Kakihana, H. *Denki Kagaku* **1978**, *46*, 553–559. (c) Brown, P. L.; Ellis, J.; Sylva, R. N. *J. Chem. Soc., Dalton Trans.* **1983**, 2001–2004.

(20) Faure, R.; Bertin, F.; Loiseleur, H.; Thomas-David, G. *Acta Crystallogr., Sect. B* **1974**, *30*, 462–467.

(21) Nakamoto, K.; Margoshes, M.; Rundle, R. E. *J. Am. Chem. Soc.* **1955**, *77*, 6480–6486.

(22) Becker, E. D. *High Resolution NMR, Theory and Chemical Applications*, 2nd ed.; Academic Press: New York, 1980.

Table VI. Selected Bond Distances (Å) and Bond Angles (deg) for $[(HB(pz)_3)BeOH]_3$ (5)

Bond Distances			
O(1)-Be(1)	1.595(4)	O(1')-Be(1)	1.581(4)
N(1)-N(2)	1.361(3)	N(1)-Be(1)	1.742(4)
N(2)-B(1)	1.544(4)	N(3)-N(4)	1.363(3)
N(3)-B(1)	1.535(4)	N(4)-Be(1)	1.741(4)
N(5)-N(6)	1.349(3)	N(5)-B(1)	1.539(4)
Bond Angles			
Be(1)-O(1)-Be(1'')	127.0(2)	N(2)-N(1)-Be(1)	123.5(2)
N(1)-N(2)-B(1)	122.8(2)	N(4)-N(3)-B(1)	124.6(2)
N(3)-N(4)-Be(1)	122.1(2)	N(6)-N(5)-B(1)	122.9(2)
N(2)-B(1)-N(3)	109.6(2)	N(2)-B(1)-N(5)	110.7(3)
N(3)-B(1)-N(5)	111.2(3)	O(1)-Be(1)-O(1')	108.8(2)
O(1)-Be(1)-N(1)	114.1(2)	O(1)-Be(1)-N(4)	108.0(2)
O(1')-Be(1)-N(1)	110.4(2)	O(1')-Be(1)-N(4)	116.0(2)
N(1)-Be(1)-N(4)	99.5(2)		

Discussion

Extraction of Group 2 Metal Ions. Using the data on the extraction of Mg^{2+} and Ca^{2+} with $[HB(pz)_3]^-$ and the extraction of Be^{2+} and Mg^{2+} with $[B(pz)_4]^-$ shown in Figure 1, the plot of logarithmic distribution ratio of the metal (log D) vs pH gives a slope of 2. This implies that the $[H_nB(pz)_{4-n}]_2M$ chelates are formed as described in eq 3 and extracted into the organic phase. Thus, the extracted species of these systems are identical with the complexes synthesized for X-ray crystallography.

When 1×10^{-4} M of Be^{2+} is extracted with $[HB(pz)_3]^-$ from aqueous solution without buffer, the slope of the log D vs pH plot is 2. The slope, however, is reduced to 1 in the presence of 1×10^{-2} M acetate buffer. Although the principal extracted species is $[HB(pz)_3]_2Be$, the formation is probably affected by complexation between Be^{2+} and acetate ions.

The extracted species of Be^{2+} and Mg^{2+} with $[H_2B(pz)_2]^-$, Sr^{2+} with $[HB(pz)_3]^-$, and Ca^{2+} with $[B(pz)_4]^-$ seem also to be $[H_nB(pz)_{4-n}]_2M$. Trofimenko has reported the precipitation of the last two complexes from the concentrated aqueous solutions.[9]

The extractability and selectivity of poly(pyrazolyl)borates presented in Figure 1 are apparently strange in the following two respects. The first point is the difference in selectivity of $[HB(pz)_3]^-$ and $[B(pz)_4]^-$ for large metal ions. It is reasonable that $[HB(pz)_3]^-$ has a higher extractability for Mg^{2+}, Ca^{2+}, and Sr^{2+} than $[H_2B(pz)_2]^-$, since $[HB(pz)_3]^-$ can act as a tridentate ligand and form six-coordinate $[H_nB(pz)_{4-n}]_2M$. *Then, why does not $[B(pz)_4]^-$ extract Ca^{2+} and larger metal ions*? The basicity of donor atoms of $[HB(pz)_3]^-$ and $[B(pz)_4]^-$ should not differ so much, because the difference in pK_{a1} is as little as 0.86. Actually, the difference in the pH values at half extraction for Mg^{2+} with these ligands is only 1.04. *Tetrakis(pyrazolyl)borate is the first chelating ligand known to us which can extract Mg^{2+} quantitatively around neutral pH but can barely extract Ca^{2+}.* Such high selectivity for Mg^{2+} over Ca^{2+} has not been attained by conventional chelating ligands.

The other question concerns the stability of beryllium complexes. The small size of Be^{2+} lends itself to a four-coordination complex. When $[Be]_i$ is 1×10^{-4} M, the extracted species are $[H_nB(pz)_{4-n}]_2Be$, in which the ligands are bidentate. While 1×10^{-2} M $[B(pz)_4]^-$ and $[HB(pz)_3]^-$ extract Be^{2+} quantitatively, the same concentration of $[H_2B(pz)_2]^-$ extracts only 24% of $[Be]_i$. This suggests that the stability of $[H_2B(pz)_2]_2Be$ is low. When $[Be]_i$ is above 1×10^{-2} M, the dominant species of beryllium in the aqueous phase around pH 5 is $[BeOH]_3^{3+}$.[19] Tetrakis(pyrazolyl)borate forms $[B(pz)_4]_2Be$ even in this condition. Tris(pyrazolyl)borate does not substitute the bridged hydroxide, forming $[(HB(pz)_3)BeOH]_3$. *Hence, the stability of the bisligand complexes increases in the order $[H_2B(pz)_2]_2Be < [HB(pz)_3]_2Be < [B(pz)_4]_2Be$.*[23] *This order of complex stability is quite the reverse of that expected on the basis of the basicity of donor atoms.* The basicity increases in the order $[B(pz)_4]^- < [HB(pz)_3]^- < [H_2B(pz)_2]^-$, since pK_{a1} increases in this order.

Examination of the structures of extracted species is essential in order to elucidate the above-mentioned problems.

Table VII. Mean Dimensions (Å or deg) of Chelate Rings in $[HB(pz)_3]_2Mg$ (1), $[HB(pz)_3]_2Ca$ (2), $[B(pz)_4]_2Mg$ (3), $[B(pz)_4]_2Be$ (4), and $[(HB(pz)_3)BeOH]_3$ (5)

	1	2	3	4	5
M-N1	2.19(3)	2.44(2)	2.16(3)	1.70(2)	1.74(1)
N1-N2	1.36(1)	1.36(1)	1.37(1)	1.37(1)	1.36(1)
N2-B	1.54(1)	1.54(1)	1.55(1)	1.54(1)	1.54(1)
N1···N1	2.94(4)	3.11(6)	2.91(1)	2.67(1)	2.66(1)
M···B	3.24(1)	3.46(1)	3.24(1)	3.08(2)	3.17(1)
N1-M-N1	84.7(2.0)	79.2(2.1)	84.7(1.1)	103.2(0.6)	99.5(0.2)
M-N1-N2	118.2(0.7)	118.2(0.6)	119.5(1.4)	121.6(0.8)	122.8(0.7)
N1-N2-B	120.7(0.6)	122.8(0.4)	119.5(2.1)	121.7(0.8)	123.7(0.9)
N2-B-N2	108.9(1.2)	110.3(0.5)	108.7(1.3)	108.4(0.5)	109.6(0.2)

Chart I

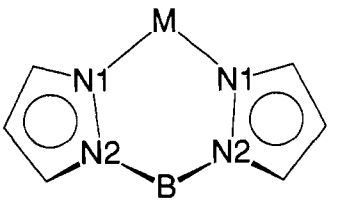

Selectivity for Six-Coordinate Metal Ions. The ^1H NMR spectra of **1** and **2** in $CDCl_3$ at 25 °C show that the pyrazolyl rings are equivalent. A 3/1 pattern is observed in the spectrum of **3**. These facts suggest that solution structures of **1–3** are similar to the structures in solid state. Exchange of the coordinated and noncoordinated pyrazolyl rings in **3** is slow on the NMR time scale at ambient temperature.

In complexes **1–3**, both ligands are tridentate and adopt a mutually staggered conformation. The pyrazolyl rings are planar, of which carbon and hydrogen atoms are oriented radially away from the B–M–B axis. This structure is quite favorable for forming a six-coordinate complex, since the increase in strain energy[1] accompanying the complex formation should be fairly small. This is especially true for $[HB(pz)_3]^-$. Tris(pyrazolyl)borate can adopt a conformation suitable for tridentate coordination without severe intraligand contact. The increase in strain energy is small when the free ligand is taken from its lower strain energy state and coordinated to a metal ion. Further, the mutually staggered conformation prevents the interligand contact, favoring formation of the six-coordinate complex. According to the phraseology by Hancock and Martell,[1] it can be said that $[HB(pz)_3]^-$ is sterically efficient to occupy a six-coordination. This steric advantage contributes largely to formation of six-coordinate $[H_nB(pz)_{4-n}]_2M$. The $[H_nB(pz)_{4-n}]_2M$ is an unusual example of group 2 metal complexes which contain only nitrogen donors and are stable in aqueous solution.[16] The basicity of donor atoms of $[H_2B(pz)_2]^-$ is higher than that of $[HB(pz)_3]^-$ and $[B(pz)_4]^-$. However, a six-coordinate $[[H_2B(pz)_2]_3M]^-$ is not formed, judging from the observation that addition of a bulky quaternary ammonium salt did not improve the E %. The formation of $[[H_2B(pz)_2]_3M]^-$ is not favored electrostatically and is sterically disadvantageous because of interligand contact.

While the structures of **1–3** resemble one another, distinct differences are recognized in the dimensions of the chelate rings. Table VII compiles the mean dimensions of chelate rings of **1–5**;

(23) The "stability" means the formation constant of poly(pyrazolyl)borate complexes from M^{2+} and $[H_nB(pz)_{4-n}]^-$. Although the formation constants should be measured, we have not succeeded in the measurement because of decomposition of the ligands in aqueous solution. The increasing order of stability is the logical conclusion on the basis of the observation of extraction and preparation of these complexes.

the labeling of atoms in the chelate ring is given in Chart I. The M–N1 distance is nearly equal to the sum of Shannon's ionic radii: 1.73 Å for Be–N, 2.18 Å for Mg–N, and 2.46 Å for Ca–N.[24] The bite size (N1···N1 distance) of $[HB(pz)_3]^-$ in **2** is larger than that in **1**. Deformation to widen the bite size is necessary when $[HB(pz)_3]^-$ coordinates to a large ion such as Ca^{2+}. The deformation is the opening of the tripod of pyrazolyl rings and is realized chiefly by increasing the bond angles of N1–N2–B and N2–B–N2. However, because of the limitation in deformation, the N1–M–N1 bond angle is considerably smaller than 90° and the trigonal distortion of **2** is enhanced.

The dimensions of the chelate rings of $[HB(pz)_3]^-$ (**1**) and $[B(pz)_4]^-$ (**3**) are practically the same. The noncoordinated pyrazolyl group has no significant effect on the chelate ring structure of Mg^{2+} complexes. However, when $[B(pz)_4]^-$ coordinates to Ca^{2+}, opening the tripod of pyrazolyl rings must cause severe steric contact between the coordinated and noncoordinated pyrazolyl rings, so that the increase in strain energy accompanying complexation becomes large. Consequently, the stability of six-coordinate $[B(pz)_4]_2Ca$ should be very low, and significant extraction of Ca^{2+} does not occur. In other words, because it is quite hard for $[B(pz)_4]^-$ to open the bite size up to 3.1 Å in a tridentate fashion, the formation of $[B(pz)_4]_2Ca$ is unfavorable. In this regard, the average bite sizes of tridentate $[B(pz)_4]^-$ in previously reported complexes are smaller than 3.0 Å.[6]

Stability of Beryllium Complexes. The only reported beryllium complexes of poly(pyrazolyl)borates are $[HB(3\text{-}Bu^tpz)_3]BeX$ (X = Br, H, etc.), which have been prepared in ethanol by Han and Parkin.[18] The average bite size in these complexes is as small as 2.73–2.79 Å. The bulky *tert*-butyl group usually hinders formation of the bisligand complex.[25] When there are no bulky substituents in the 3-position of the pyrazolyl ring, formation of $[H_nB(pz)_{4-n}]_2Be$ is preferred, of which poly(pyrazolyl)borates are bidentate.

The ^1H NMR measurement reveals that the structures of **4** and **5** in $CDCl_3$ are similar to those in solid state. The spectrum of **4** has a 1/1 pattern. The four coordinated and four noncoordinated pyrazolyl rings would be equivalent because of a boat–boat flip of the BeN_4B rings. Exchange of the coordinated and noncoordinated rings seems a slow process. A 2/1 pattern is observed in the spectrum of **5**. This indicates that the six pyrazolyl rings coordinated to Be^{2+} are equivalent and that exchange of the coordinated and noncoordinated rings is slow. In the solid state, the $[BeOH]_3^{3+}$ ring has a chair conformation, and the symmetry of **5** is as low as C_3. The $[BeOH]_3^{3+}$ ring in solution either has a planar conformation or is flipping rapidly.[19b]

The conformation of $[B(pz)_4]^-$ in **4** is popular in tetrakis(pyrazolyl)borate complexes where this ligand is bidentate.[5b,c,6d,7] A similar conformation is also observed in crystals of sodium and potassium salts of $[B(pz)_4]^-$.[26] The strain energy of free $[B(pz)_4]^-$ is lowest in this conformation because the steric contact among the pyrazolyl rings can be minimized. In the solid state of sodium and potassium salts, the distance between the closest nitrogen donors is 3.03–3.06 Å.[26] The N···N distance (bite size) is reduced to 2.66 Å when the ligand coordinates to Be^{2+} bidentately. This change in conformation would cause steric contact between the coordinated pyrazolyl rings. For $[B(pz)_4]^-$, however, the increase in strain energy caused by the coordination should be relatively small and sufficiently compensated with the favorable free energy change of the chelate ring formation.

While the structures of free $[HB(pz)_3]^-$ and $[H_2B(pz)_2]^-$ have not been reported yet, their pyrazolyl rings may be more remote from each other than the pyrazolyl rings of $[B(pz)_4]^-$. Figure 7 shows the space-filling models of structures of $[HB(pz)_3]^-$ in **5** and $[B(pz)_4]^-$ in **4**. The coordination around the boron atom of $[B(pz)_4]^-$ is obviously very crowded. In contrast, there is much space around the boron atom of $[HB(pz)_3]^-$. It is anticipated that the conformations of free $[HB(pz)_3]^-$ and $[H_2B(pz)_2]^-$ substantially differ from the conformations of these ligands when coordinated to Be^{2+} and that the strain energy of free $[HB(pz)_3]^-$ and $[H_2B(pz)_2]^-$ is lower than that of $[B(pz)_4]^-$. Hence, the increase in strain energy accompanying the formation of $[H_nB(pz)_{4-n}]_2Be$ becomes larger for $[HB(pz)_3]^-$ and $[H_2B(pz)_2]^-$ than does the increase for $[B(pz)_4]^-$. This is the reason for the lower stability of bisligand beryllium complexes of $[HB(pz)_3]^-$ and $[H_2B(pz)_2]^-$.

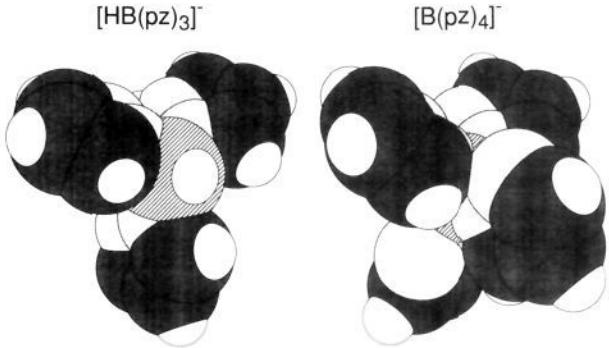

Figure 7. Space-filling view of $[HB(pz)_3]^-$ in **5** and $[B(pz)_4]^-$ in **4**.

Control of Complex Structure. Thus far it has been discussed how the intraligand contact influences the stability of complexes of the same structure. The intraligand contact further results in very different structures of complexes of the same metal with $[B(pz)_4]^-$ and $[HB(pz)_3]^-$. The first clear example has been shown with lead(II) complexes by Reger et al.[5c] They have prepared $[HB(pz)_3]_2Pb$, $[HB(3,5\text{-}Me_2pz)_3]_2Pb$, and $[B(pz)_4]_2Pb$ in water and determined the X-ray crystal structures of these complexes. The geometry about the lead atom in $[HB(pz)_3]_2Pb$ is a capped octahedron, with the lone pair on the metal located in the capping position of the triangular face. The geometry about the lead atom in $[HB(3,5\text{-}Me_2pz)_3]_2Pb$ is a trigonally distorted octahedron, where the lone pair is stereochemically inactive. The ligands in these two complexes are tridentate. On the other hand, the geometry about the lead atom in $[B(pz)_4]_2Pb$ is a distorted pseudotrigonal bipyramid with the lone pair on the lead atom occupying an equatorial site. The $[B(pz)_4]^-$ acts as a bidentate ligand. The structures of these three complexes in solution appear similar to the structures in solid state judging from the NMR data. Reger pointed out that the intraligand contact among the pyrazolyl rings of $[B(pz)_4]^-$ favors bidentate coordination for the large size of lead(II). If the ligand is tridentate, the noncoordinated pyrazolyl ring cannot avoid unfavorable steric interactions with the coordinated rings. Actually, the average bite size is 3.11 Å for $[HB(pz)_3]_2Pb$ and 3.18 Å for $[HB(3,5\text{-}Me_2pz)_3]_2Pb$ according to their data. These bite sizes are as large as the bite size of **2** observed in this work. Therefore, it is reasonable that $[B(pz)_4]^-$ cannot open the bite size enough to coordinate trigonally to the lead atom.

Similar phenomena have been found for the tin(II) complexes.[5a,b] In both solution and solid phases, the geometry about the tin atom in $[B(pz)_4]_2Sn$ is a trigonal bipyramid with each ligand being bidentate. The ^{119}Sn NMR data, however, indicated that $[HB(pz)_3]_2Sn$ may be a five-coordinate complex in solution. The X-ray crystallography for $[HB(3,5\text{-}Me_2pz)_3]_2Sn$ has shown that the geometry around tin(II) is approximately octahedral and that one $[HB(3,5\text{-}Me_2pz)_3]^-$ is bidentate and the other is tridentate.[5a] The average bite size of the tridentate $[HB(3,5\text{-}Me_2pz)_3]^-$ is 3.07 Å, which is again too large for $[B(pz)_4]^-$ to adopt.

(24) Shannon, R. D. *Acta Crystallogr., Sect. A* **1976**, *32*, 751–767. The radius of the nitrogen atom is taken as 1.32 Å of four-coordinate N^{3-}.

(25) (a) Calabrese, J. C.; Trofimenko, S.; Thompson, J. S. *J. Chem. Soc., Chem. Commun.* **1986**, 1122–1123. (b) Trofimenko, S.; Calabrese, J. C.; Thompson, J. S. *Inorg. Chem.* **1987**, *26*, 1507–1514.

(26) Lopez, C.; Claramunt, R. M.; Sanz, D.; Foces, C. F.; Cano, F. H.; Faure, R.; Cayon, E.; Elguero, J. *Inorg. Chim. Acta* **1990**, *176*, 195–204.

The above discussion is on the structure change for the complexes of large metal ions. The results of this work demonstrate for the first time that $[HB(pz)_3]^-$ and $[B(pz)_4]^-$ can also produce totally different structures of complexes of a very small metal ion. In aqueous solution of Be^{2+}, polymeric species, such as $[BeOH]_3^{3+}$ or $[Be_2OH]^{3+}$, are formed in the course of hydrolysis.[19] The structure of beryllium complexes of poly(pyrazolyl)borates depends upon competition of poly(pyrazolyl)borates and hydroxide ions for coordination sites of Be^{2+}. Tetrakis(pyrazolyl)borate effectively excludes hydroxide ions and forms $[B(pz)_4]_2Be$, since the conformation change of the ligand molecule from the free state to the coordinated state to Be^{2+} is accompanied with only a small increase in strain energy. The increase in strain energy is considerable for $[HB(pz)_3]^-$ to coordinate to Be^{2+} and counteracts the advantageous entropy change of chelate formation. Hydrotris(pyrazolyl)borate cannot substitute hydroxide ions bound to Be^{2+} effectively. As a consequence, $[HB(pz)_3]^-$ forms $[HB(pz)_3]_2Be$ when the dominant dissolved species of beryllium is Be^{2+} and forms $[(HB(pz)_3)BeOH]_3$ when the dominant species is $[BeOH]_3^{3+}$.

Conclusion

Stability and structure of poly(pyrazolyl)borate complexes of group 2 metals are controlled by intraligand contact between pyrazolyl rings bonded to the central boron atom. Tris(pyrazolyl)borate can coordinate to large metal ions in a tridentate fashion by opening the tripod of pyrazolyl rings. For $[B(pz)_4]^-$, the tridentate coordination to large metal ions is unfavorable because of steric contact between the coordinated and noncoordinated pyrazolyl rings. Tetrakis(pyrazolyl)borate preferentially acts as a bidentate ligand to avoid the intraligand contact. Consequently, while $[HB(pz)_3]^-$ readily forms six-coordinate $[HB(pz)_3]_2Ca$, formation of an analogous complex of $[B(pz)_4]^-$ is unfavorable.

For the small size of Be^{2+}, all of $[H_2B(pz)_2]^-$, $[HB(pz)_3]^-$, and $[B(pz)_4]^-$ prefer bidentate coordination. When these ligands coordinate to Be^{2+}, the coordinated pyrazolyl rings approach each other and cause intraligand contact. The increase in strain energy accompanying the complex formation is small for $[B(pz)_4]^-$, of which steric crowding around the boron atom favors the bidentate coordination in a compact arrangement. Thus, stable four-coordinate $[B(pz)_4]_2Be$ is formed. The stability of $[H_nB(pz)_{4-n}]_2Be$ decreases as the steric crowding around the boron atom is relieved. Tris(pyrazolyl)borate is a somewhat weaker ligand for Be^{2+} than hydroxide ion and forms $[HB(pz)_3]_2Be$ or $[(HB(pz)_3)BeOH]_3$ according to the dominant species of beryllium in aqueous solution.

The results of this work demonstrate a new mode of ion size discrimination by chelating ligands. In this mode, selectivity of ligands for metal ions can be readily changed by introduction of substituents on the central atom. Furthermore, such high selectivity of $[B(pz)_4]^-$ for Mg^{2+} over Ca^{2+} has not been attained by conventional chelating ligands. The qualitative discussion in this paper will be quantified on the basis of molecular mechanics or other computational chemistry.

Acknowledgment. We are grateful to Prof. Yasuo Hata (Kyoto University) for helpful discussion. This research was supported by a Grant-in-Aid (No. 03453042) from the Ministry of Education, Science and Culture, Japan.

Supplementary Material Available: Tables of crystallographic details, positional and thermal parameters, temperature factors, bond distances, and bond angles for **1–5** (52 pages); listing of observed and calculated structure factor amplitudes for **1–5** (99 pages). Ordering information is given on any current masthead page.